Cartilage lamina splendens inspired nanostructured coating for biomaterial lubrication

Wan, Hongping; Ren, Ke; Kaper, Hans J; Sharma, Prashant K

Published in:
Journal of Colloid and Interface Science

DOI:
10.1016/j.jcis.2021.03.052

Publication date:
2021

Journal of Colloid and Interface Science 594 (2021) 435–445

Contents lists available at ScienceDirect

Journal of Colloid and Interface Science

journal homepage: www.elsevier.com/locate/jcis

Regular Article

Cartilage lamina splendens inspired nanostructured coating for biomaterial lubrication

Hongping Wan [a,b,*,1], Ke Ren [b,1], Hans J. Kaper [b], Prashant K. Sharma [b,*]

[a] College of Veterinary Medicine, Sichuan Agricultural University, Department of Animal and Plant Quarantine, Chengdu 611130, China
[b] University of Groningen and University Medical Center Groningen, Department of Biomedical Engineering, Antonius Deusinglaan 1, 9713 AV Groningen, the Netherlands

GRAPHICAL ABSTRACT

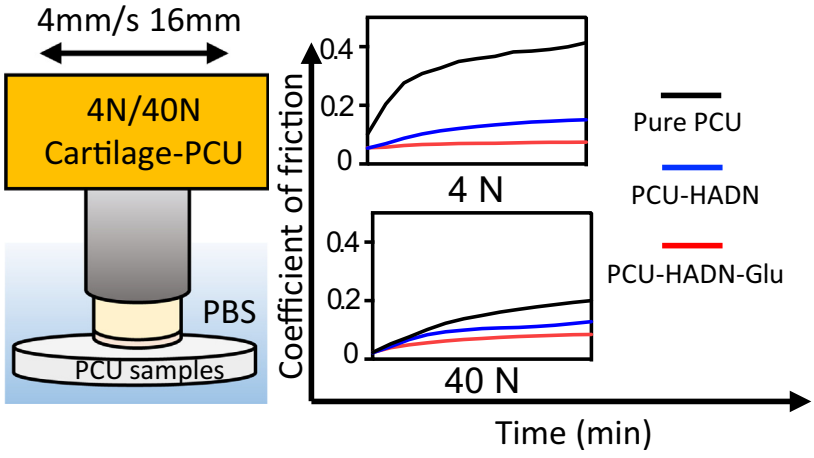

ARTICLE INFO

Article history:
Received 13 October 2020
Revised 8 March 2021
Accepted 9 March 2021
Available online 17 March 2021

Keywords:
Lubrication
Cartilage
Implant
Boundary lubrication
Coating

ABSTRACT

Biomaterials that are used in biological systems, such as polycarbonate urethane (PCU) knee joint implants and contact lenses, generally lack lubrication. This limits their integration with the body and impedes their function. Here, we propose a nanostructured film based on hydrophilic polysaccharide hyaluronic acid conjugated with dopamine (HADN) and zwitterionic reduced glutathione (Glu), which forms a composite coating (HADN-Glu) to enhance the lubrication between cartilage and PCU. HADN was synthesized by carbodiimide chemistry between hyaluronic acid and dopamine and deposited on PCU surface under mild oxidative conditions. Then, zwitterionic peptide-reduced glutathione was bio-conjugated to HADN, forming a lubrication film. Analysis based on X-ray photoelectron spectroscopy (XPS), atomic force microscopy (AFM) and wettability indicated that HADN and Glu had grafted successfully onto the PCU surface. Measurements of the coefficient of friction (COF), friction energy dissipation and cartilage roughness indicated that cartilage was effectively protected by the high lubrication of HADN-Glu. Both at low and high applied loads, this effect was likely due to the enhanced boundary

* Corresponding authors at: College of Veterinary Medicine, Sichuan Agricultural University, Department of Animal and Plant Quarantine, Chengdu 611130, China (H. Wan); University of Groningen and University Medical Center Groningen, Department of Biomedical Engineering, Antonius Deusinglaan 1, 9713 AV Groningen, the Netherlands (P.K. Sharma).
E-mail addresses: wanwanwanhome@126.com (H. Wan), p.k.sharma@umcg.nl (P.K. Sharma).
[1] Contribute equally and share the first author.

https://doi.org/10.1016/j.jcis.2021.03.052
0021-9797/

lubrication enabled by HADN-Glu on the PCU surface. Moreover, HADN-Glu is highly biocompatible with chondrocyte cells, suggesting that this film will benefit the design of implants where lubrication is needed.

1. Introduction

Biolubrication in living systems is based on maintaining a fluid film between articulating surfaces, whose thickness dictates the lubrication mechanism [1,2]. Articular cartilage, for instance, is known to be lubricated through hydrostatic weeping lubrication [3,4] at high loads due to its biphasic structure [5,6] and through boundary lubrication at low loads during the gait cycle. Boundary lubrication is attributed to Lamina splendens, which is an acellular and non-fibrous layer [7] adsorbed on parallelly-oriented collagen fibrils at the surface of the cartilage. The constituents of lamina splendens – hyaluronic acid (HA) [8], zwitterionic phospholipids [5,9,10] and proteoglycan-4 (PRG4) [11–16] separately or simultaneously in pairs [9,16] – are thought to be responsible for boundary lubrication at low loads and low speeds. The extremely low kinetic coefficient of friction (COF $\mu \sim 0.005$) [10,17] observed in the knee joint is due to lubricating molecules, whereby HA increases the viscosity of the synovial fluid and works synergistically with glycoprotein and zwitterionic lipid to enhance boundary lubrication [18].

The biolubrication mechanism completely changes when a biomaterial is introduced into otherwise healthy biological surroundings, e.g., the introduction of an artificial meniscus in the knee joint [4] or a contact lens between the cornea and the eyelid [19,20]. The poor adsorption of macromolecules like HA on biomaterials leads to a different lubrication mechanism [21]. Caligaris et al. has shown that shifting from fluid film lubrication to boundary lubrication with high friction could happen in the fiction system of cartilage-glass [22]. Surface modification technology has been used to improve the tribological performance of medical devices. A coating of poly (2-methacryloyloxyethyl phosphorylcholine-*co*-*n*-butyl methacrylate) [poly(MPC-*co*-BMA)] on polyurethane (PU) surface yields low friction due to sufficient hydration and boundary lubrication [23]. The tribological and chemical characteristics of poly (MPC-*co*-BMA) has increased the efficacy of PU for clinical applications. Enhanced capacity of water retention due to promoting the adsorption of lubricious molecule shows some effects on contact lenses [8], but the lubrication function remains unclear. Most studies have focused on the physical–chemical properties of the structure of materials rather than testing the function with real tissue. Being a specialized tissue with a biphasic structure, cartilage is known to react differently to different loading conditions. Polycarbonate urethane (PCU) [24] is considered a good candidate for orthopedic implants as they have been demonstrated to possess a unique combination of toughness, durability, biostability and biocompatibility. The PCU used for meniscus implant demonstrate similar mechanical properties, e.g., its stiffness is similar to natural meniscus at body temperature. But its lubrication properties against cartilage are suboptimal [24]; during the swing phase of the gait cycle the PCU-cartilage friction is an order of magnitude higher than meniscus-cartilage friction [4], which can potentially cause cartilage damage [4] in the long run.

Taking cues from the native lubrication film of lamina splendens [25], in which hydrophilic and zwitterionic molecules such as hyaluronic acid (HA), protein and lipid work synergistically and yield low friction [26,27], we designed a biomimetic film for the PCU surface. HA, the only polysaccharide in synovial fluid and lamina splendens, provides effective lubrication in the knee joint, but it does not easily adsorb to biomaterials such as PCU. HA can be made adhesive by conjugating it with 3,4-dihydroxy-L-phenylalanine (DOPA), whose *ortho*-dihydroxy phenyl (catechol) group acts as an adhesive on various inorganic/organic surfaces [28] and can be readily coupled to the carboxyl residues on HA via carbodiimide chemistry [29,30]. Dopamine-conjugated HA (HADN) is adhesive in nature and has been used in the past for increasing cell responsiveness [30]. Zwitterionic molecules containing both negatively and positively charged groups have shown antifouling properties [31], and zwitterionic hydrogels [32] or crosslinked co-polymer brushes have shown high lubricity [33]. Zwitterionic lipids, together with HA, could enhance the lubrication due to their strong water immobilization [34].

Glutathione (Glu) is a natural tripeptide composed of glutamic acid, cysteine and glycine; It has a zwitterionic pair and abundant polar groups providing strong interaction with water [35]. The thiol (-SH) group of cysteine is easy to bioconjugate to HADN via Michael addition or Schiff base reactions, and forms the Glu-HADN composite film spontaneously. Glu has been shown to couple to HA, resulting in better antifouling performance induced by zwitterionic Glu with strong surface hydration [36]. However, the lubrication properties of Glu coupled to HADN have never been investigated.

We hypothesize that the adhesive properties of HADN synergize with the zwitterionic nature of Glu and the Glu-HADN composite film on PCU to enhance lubrication against cartilage. In the present study, physisorption of HADN onto PCU surface was followed by Glu modification of the HA backbone of HADN molecules. HADN was synthesized via a simple carbodiimide reaction and then attached to PCU under mild alkaline conditions. Then reduced Glu was coupled to HADN via Michael addition. X-ray photoelectron spectroscopy (XPS), atomic force microscopy (AFM), contact angle measurements were used to characterize the physicochemical surface properties. Furthermore, the lubrication enhancement was evaluated by a universal mechanical testing machine (UMT-3) with a PCU-cartilage lubrication system. The lubrication mechanism was also analyzed (Scheme 1).

2. Materials and methods

2.1. Synthesis of HADN

Hyaluronic acid (Kraeber & Cogmbh, Germany) of 600 kDa was coupled to dopamine hydrochloride (CAS no. 62-31-7, certified reference grade material, Sigma-Aldrich) by active agent of N-(3-Dimethylaminopropyl)-*N*-ethylcarbodiimide hydrochloride (EDC, purity $\geq$ 98.0% (AT), Sigma-Aldrich, CAS no. 25952-53-8) (Fig. 1a) as described previously [37]. Briefly, 40 mg HA was dissolved in 8 ml Phosphate Buffer solution (PBS) at pH 5 adjusted by hydrochloric acid (HCl, CAS no. 7647-01-0, ACS reagent grade, Sigma-Aldrich). Then 13.5 mg EDC and 19 mg dopamine were added to the HA solution at pH 5 and allowed to react for 5 h. The reaction was protected with nitrogen. Unreacted chemicals and byproducts were removed by extensive dialysis (molecular weight cut-off: 3500 Da, spectrum medical industries, USA) for 3 days in deionized water (pH 5), which was exchanged every 3 h. The conjugate product then was lyophilized and stored at 4 °C in a moisture-free desiccator for further use.

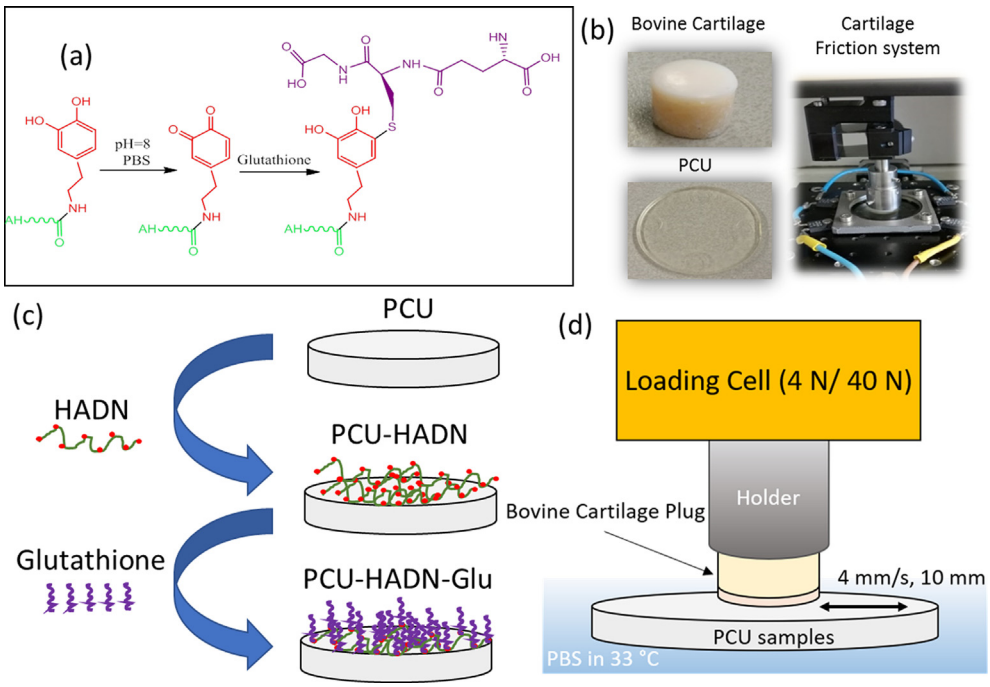

Scheme 1. Schematic representation of of PCU-cartilage friction system with or without HADN-Glu coating.

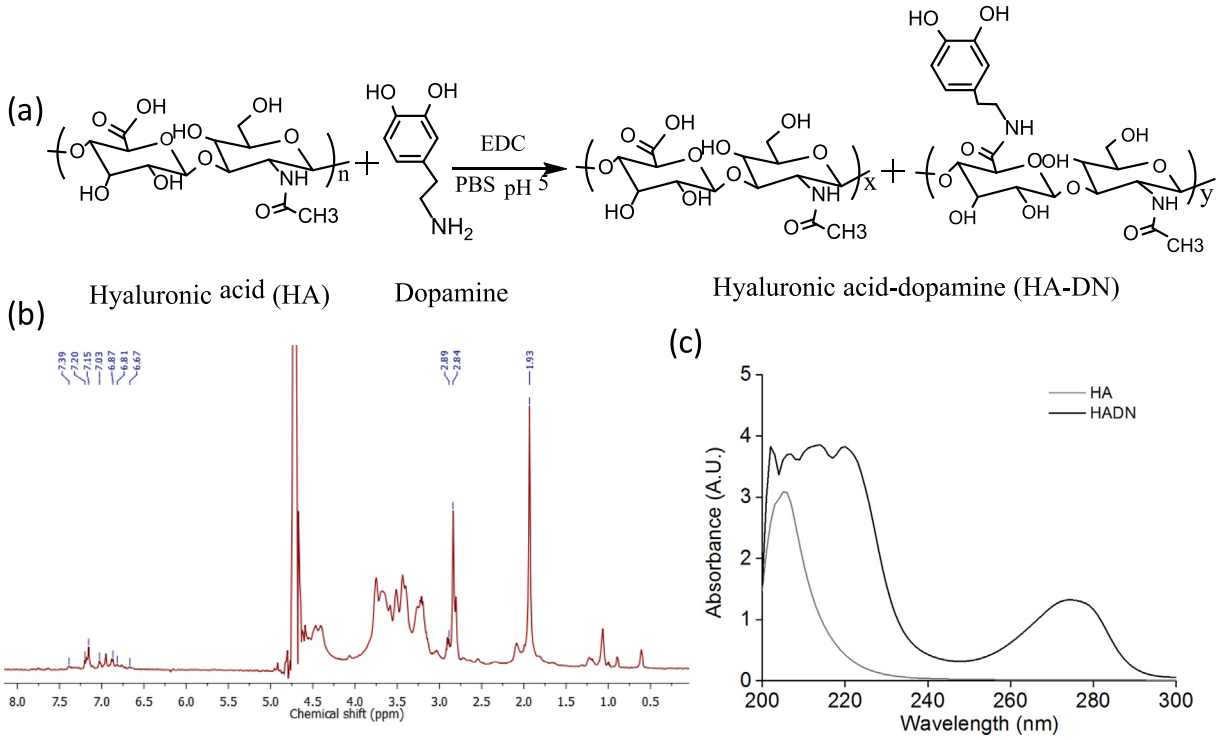

Fig. 1. Synthesis and structure of HADN. (a) The schematic representation of the procedure to synthesize HADN. (b) The H-NMR spectrum of HADN. (c) UV–Vis spectra of the conjugate (HADN) and the control (HA).

Nuclear Magnetic Resonance (NMR) and Ultraviolet spectrophotometry (Uv–vis) were used to characterize HADN. A lyophilized sample was dissolved in deuterated water at 5 mg/ml for ^{1}H NMR (Bruker Avance, 400 MHz) analyses. Dopamine solution with various concentrations from 0.1 mM to 1 mM in PBS were prepared and their spectrum absorbance at 280 nm was measured by Uv–Vis spectrum (Beckman, USA) with a 1 cm wide cuvette. The standard curve was then calculated by linear fitting. The absorbance at 280 nm of 1 mg/ml HADN was used to calculate the conjugation degree by comparing it with the standard curve.

2.2. PCU surface modification

All the PCU disks were cleaned with *n*-hexane, then extensively washed with ethanol and milli-Q water. 20 mg HADN conjugate was dissolved in 5 ml PBS buffer (pH = 8, 10 mM) to a final concen-

tration about 4 mg/ml. Then cleaned bare PCU slides were immersed in the HADN solution at room temperature overnight (37 °C, 12 h) to allow physisorption. The PCU surface was coated with HADN (now called PCU-HADN) and washed with Milli-Q water to remove the free HADN, dried in a stream of nitrogen and stored at 4 °C until used. For PCU-HADN modification with Glu, 20 mg Glu (CAS no. 70–18-8, BioRegent, purity ≥ 98.0%, Sigma-Aldrich) was dissolved in 10 ml PBS buffer (pH = 8, 10 mM) to a final concentration about 2 mg/ml. Before dissolving Glu, PBS was degassed by nitrogen for 2 h to prevent disulfide bond (—S—S—) formation between each Glu monomer. Then the PCU-HADN was immersed in Glu solution for another 12 h at room temperature to allow chemisorption of Glu via Michael addition (now called PCU-HADN-Glu). The HADN-Glu coating was washed in milli-Q water to remove the free Glu, then dried in a stream of nitrogen and stored at 4 °C until used.

2.3. Surface characterization

The surface roughness of PCU samples was measured by atomic force microscopy (AFM) (Nanoscope IV Dimensiontm 3100, USA) equipped with a dimension hybrid XYZ SPM scanner head (Veeco, New York, USA). A scan area of 20 × 20 μm^2, a scanning frequency of 1 Hz and a scanning resolution of 512 × 512 pixels was used in contact mode in air with a constant normal force of 5 nN. Water contact angle measurements were performed at room temperature using an OCA 15 plus goniometer (DataPhysics Instruments, Germany). The values were obtained by the sessile drop method. The used liquid was ultrapure water and the drop volume was 5 μl. At least three measurements were carried out on each sample.

2.4. X-ray photoelectron spectroscopy

The elemental composition of the PCU, PCU-HADN, and PCU-HADN-Glu surface was determined using XPS (S-Probe, surface science instruments, mountain view, CA, USA). XPS detects only the top 10 nm of the surface. First, the PCU samples were moved to XPS pre-vacuum chamber. Then a vacuum of 10^{-7} Pa was generated. X-rays (10 Kv, 22 mA), spot size 250 × 1000 μm, were produced using an aluminum anode. Photoelectrons in the binding energy range of 1–1100 eV were detected at low resolution. The area under each peak yield elemental surface concentrations for C, N, O. Correction was applied with the help of sensitivity factors provided by the manufacturer.

2.5. Cartilage friction against PCU-HADN-Glu.

Fresh osteochondral plugs (12 mmϕ) bored out of the femoral heads of bovine stifle joints (from 2 year-old bulls) were mounted on the universal mechanical tester (UMT-3, CETR Inc., USA). The counter surface was either PCU, PCU-HADN, or PCU-HADN-Glu submerged in PBS at 33 °C. To mimic the swing and stance phase of the gait cycle, loads of 4 N and 40 N were applied, giving rise to an average contact pressure of 0.4 and 4 MPa, respectively. A sliding velocity of 4 mm/s was used over a sliding distance of 10 mm for 1 h, resulting in 720 cycles during each tribological test [4,38]. Average dynamic COF, friction energy dissipation, and dynamic creep were measured. Average dynamic COF was obtained by calculating the mean level of COF (friction force/normal force) in each cycle. To simplify the display of results, average COF was then calculated for every 5 min interval, e.g. 0 min (cycle 0), 5 min (average from 0 to 60 cycles), 10 min (average from 61 to 120 cycles) and so on.

To determine frictional energy loss during reciprocal sliding (which plays a crucial role in understanding cartilage friction and wear [39]), we plotted frictional force as a function of distance (Ft–D). The friction force values were positive during trace but negative during re-trace. Both were shifted to positive (Fig. 3c) before calculating the area inside the loop. The area value of each friction loop (Ft–D) is the energy dissipation of each cycle, which was calculated by applying definite integral algorithm as described elsewhere [39].

2.6. Cartilage topography using atomic force microscopy

Cartilage before and after tribology measurement was fixed by paraformaldehyde (Sigma, CAS no. 30525-89-4) for 45 min at room temperature, followed by rinsing with PBS. Surface roughness and morphology was observed by AFM operating with the contact mode in air with a constant normal force of 5 nN. Bruker Cantilevers, made from silicon nitride with a spring constant of 0.06 N/m, were used in this measurement to scan the cartilage surface with a scanning resolution of 512 × 512 pixels. Data analysis was performed on NanoScope Analysis (also Bruker). To calculate surface roughness, first-order flattening was applied to all AFM images.

2.7. Evaluation of cell behavior

Chondrocytes from humans [40] were seeded onto a piece of circular glass with a diameter of 15 mm (ϕ 15 mm) that fits onto 24-cell culture plates [37,41]. The glass pieces were coated with or without layers of HADN or HADN-Glu. The procedure was the same as for the PCU treatment described above. Each sample was seeded with 5 × 10^4 cells and cultured with high glucose Dulbecco's Modified Eagle Medium (DMEM Gibco), 10% fetal bovine serum (FBS Gibco), and penicillin – streptomycin (10,000 units/mL of penicillin and 10,000 μg/mL of streptomycin, Thermo Fischer Scientific, Cat no. 15140122) at pH 7.4. After that, samples were incubated at 37 °C in a humidified atmosphere of 5% CO_2. Every 3 to 4 days, the medium was changed. Cell viability was measured using an XTT assay (Applichem A8088). Briefly, on day 1, day 3, and day 7, 300 μl of XTT reaction reagent (0.1 ml activation reagent and 5 ml XTT mixture) was added to each well after incubation at 37 °C in a humidified air atmosphere of 5% CO_2 for 3 h; the microplate reader was used to record absorbance at 485 and 690 nm. Fluorescence was measured by confocal microscopy with TRITC-phalloidin and DAPI staining, which provides a visual morphology of chondrocytes. Briefly, cells were fixed by paraformaldehyde for 15 min at room temperature, followed by washing with PBS. Then 500 μl of a mixture (TRITC-labelled phalloidin Sigma, P1951 at 2 μg/ml and DAPI, Sigma, CAS Number 28718-90-3 at 4 μg/ml in PBS) was added to each well plate. Afterward, cells were incubated for 1 h at room temperature with aluminum foil for protection from light. Finally, the 24-cell culture plate was visualized in the dark by confocal microscopy.

2.8. Statistical analysis

All data are expressed as means ± SD, calculated from three independent experiments i.e. 3 osteochondral plugs sliding against 3 different (coated or uncoated) PCU surfaces. Statistical analysis was performed with Graphad Prism version 7.0 for windows (GraphPad Software, La Joola California USA). Significant differences between groups by using two-tailed Student's t analysis, accepting significance at $p < 0.05$.

3. Results and discussion

3.1. HADN conjugation synthesis and characterization

HADN was prepared by carbodiimide chemistry with N-(3-Dimethylaminopropyl)-*N*-ethylcarbodiimide hydrochloride (EDC) coupling reaction [28,29,42,43]. A schematic representation of synthetic procedure was shown in Fig. 1a. The multiplets observed between δ = 6.7 ppm and δ = 7.0 ppm in ^{1}H NMR spectra in Fig. 1b are associated with protons of the aromatic ring [30]. Chemical shift at 2.03 ppm is associated with protons of N-$COCH_3$ [30], demonstrating that HADN conjugation was successful. The results also were confirmed by Uv–visible spectrophotometer in Fig. 1c. An absorbance band around 280 nm, the characteristic absorbance of catechol, was observed in HADN, but not in HA alone. Dopamine solutions with concentrations ranging from 0.1 mM to 1 mM in PBS were prepared. Their spectrum absorbance at 280 nm was measured by Uv–Vis spectrum. Then the standard curve was calculated by linear fitting, as shown in Fig. S1. Based on a standard curve and the A_{280} nm of the synthesized product, the conjugation was calculated as about 22%. This means that on average, every fifth carboxyl was conjugated with DN. Amidation by a carbodiimide coupling method [30] is widely used in biomaterial application because it is highly effective and reproducible. Different equivalent proportions can yield different conjugation degrees. In the present study, we chose a 22% conjugation because less than 10% is conventionally considered to be a low catechol conjugation level for a polymer. Likewise, a conjugation degree over 30% is regarded to be a high catechol conjugation for a polymer [44,45].

3.2. PCU-HADN and PCU-HADN-Glu preparation and characterization

HADN was immobilized on the PCU surface via its catechol groups, as shown schematically in Fig. 3. PCU disks were immersed in HADN under mild alkaline conditions (PBS, pH = 8) with a concentration of 4 mg/ml at room temperature for 12 h. During this period, the catechol groups form quinone groups to assist the deposition of HADN on the PCU surface (denoted as PCU-HADN) by hydrophobic interaction [46]. Reduced Glu, containing the zwitterionic pair, was grafted onto the HADN-modified PCU surface (denoted as PCU-HADN-Glu) via Michael addition.

The surface morphologies of bare PCU, PCU–HADN, and PCU-HADN-Glu were measured by AFM as shown in Fig. 2a**.** The surface of bare PCU is relatively smooth with surface roughness (R_q) around 11.6 ± 0.7 nm. After HADN modification, small but dense particles were fully covered on the PCU surface, indicating that HADN covered the PCU surface homogeneously, which could further recruit Glu onto the HADN surface. Compared to bare PCU, the roughness was slightly increased to 13.7 ± 1.0 nm on PCU-HADN, and 13.9 ± 1.1 nm on PCU-HADN-Glu, indicating that a uniform coating was obtained on the PCU surface. Although no significant difference was observed in the surface roughness between PCU-HADN and PCU-HADN-Glu, the surface morphology was different, indicating Glu adsorption onto HADN. To confirm that surface modification was successful, XPS was used to detect the chemical element changes in the substrate, as shown in Fig. 2, Fig. S2, Table 1 and Table S1. In the mild alkaline conditions, most of the catechol were oxidized to quinone (Fig. S2 and Table S1), and the percentage of O1s (C═O) was 61.4 ± 10.2%. After adsorption of Glu, the percentage of C═O was decreased to 27.8 ± 18.4%, which could have been caused by the Michael addition. C1s spectra on the surface of HADN and HADN-Glu were deconvoluted into three curves: C—C, C—N/C—O, and C═O, as shown in Table S1 and Fig. S2. Their relative percentages were also different, which could be caused by the binding of Glu. On bare PCU, the majority of the elements consisted of carbon (80.4% ± 2.9%), nitrogen (1.3% ± 0.07%), and oxygen (13% ± 1.4%). The proportions of nitrogen and oxygen increased to 7.6% ± 0.5% and 26.0% ± 1.7% after HADN modification and to 9.8% ±1.8% and 27.3% ±1.6% after HADN-Glu modification, respectively. The N/C ratio also increased from 1.6 ± 0.1% in bare PCU to 14.9 ± 0.3% in PCU-HADN and 20.5 ± 3.8% PCU-HADN-Glu. The relatively higher N content after HADN modification could be caused by the dopamine.

After Glu coupled to the HADN surface, the N percentage increased further due to the higher amount of N in Glu. The result of XPS indicated that the PCU surface was successfully modified by HADN and Glu. To characterize the wettability of PCU surface modified with HADN and HADN-Glu, the static water contact angles of bare PCU, PCU-HADN and PCU-HADN-Glu surface were measured, as shown in Fig. 2c. The bare PCU surface was slightly hydrophobic and had a water contact angle of 95.3° ± 1.3°, which decreased to 61.8° ± 4.9° and 59.7° ± 3.3° after HADN and HADN-Glu deposition on the PCU surface, respectively. Although no significant difference between PCU-HADN and PCU-HADN-Glu was observed, the slightly lower water contact angle on PCU-HADN-Glu surface could be attributed to the influence of Glu with strong hydration. Previous studies have also shown that a decrease in water contact angle results from hydrophilic compound adsorption on hydrophobic surface [36], which was confirmed in our study. From the results of AFM, XPS and water contact angle, we can infer the HADN and Glu successfully coated the PCU surface.

3.3. Lubrication of PCU-HADN-Glu against cartilage

PCU is a popular biomaterial for porous and nonporous permanent meniscus implants for the replacement of damaged meniscus [47–51]. However, its lubrication properties during the swing phase have been shown to be suboptimal [4] and need improvement. When tested with alternate swing and stance phase loads, the cartilage-PCU COF at low loads (4 N) – corresponding with the swing phase of the gait cycle – was found to be higher than during the stance phase (40 N). Even at 40 N, the COF continuously increased with time [4], thus limiting the functional longevity of PCU. In the present study, we tested cartilage friction at constant loads – either 4 N or 40 N for 60 min – which differs from the protocol used by Majd et al. [4]. Despite this different protocol, at low loads (4 N) the COF between bare PCU and cartilage increased gradually up to 0.41 ± 0.06 (Fig. 3), which is consistent with the finding of Majd et al. [4,24]. After coating the PCU with HADN, the COF decreased to a significantly lower value: 0.15 ± 0.07. Further modification with glutathione (PCU-HADN-Glu) lowered the COF even further – 0.07 ± 0.01 at the end of 60 min – indicating that the HADN-Glu coating efficiently lubricated the PCU during the swing phase.

Besides COF, the dynamic creep was also monitored in (see Fig. 4b) during the 60 min sliding. Dynamic creep is the combined effect of two processes – creep of PCU and depressurization of the cartilage due to release of interstitial fluid – as proposed by Ateshian et al. [22,52]. This is shown in Eq. (1):

$$\frac{\mu_{eff}}{\mu_{eq}} = 1 - (1-\varphi)\frac{W^p}{W} \tag{1}$$

where φ is the fraction of the contact area over the contact occurs; $1\text{-}\varphi$ is the water content of cartilage at the articular surface [53], which averages to 0.91 for normal bovine cartilage [54]; W^p/W is the interstitial fluid load support; μ_{eff} and μ_{eq} are the time-dependent and equilibrium coefficient of friction, respectively.

The frictional energy loss in the process of reciprocal sliding was calculated and is shown in Fig. 3c and d. Frictional energy can be dissipated as heat, but part of the energy could also be

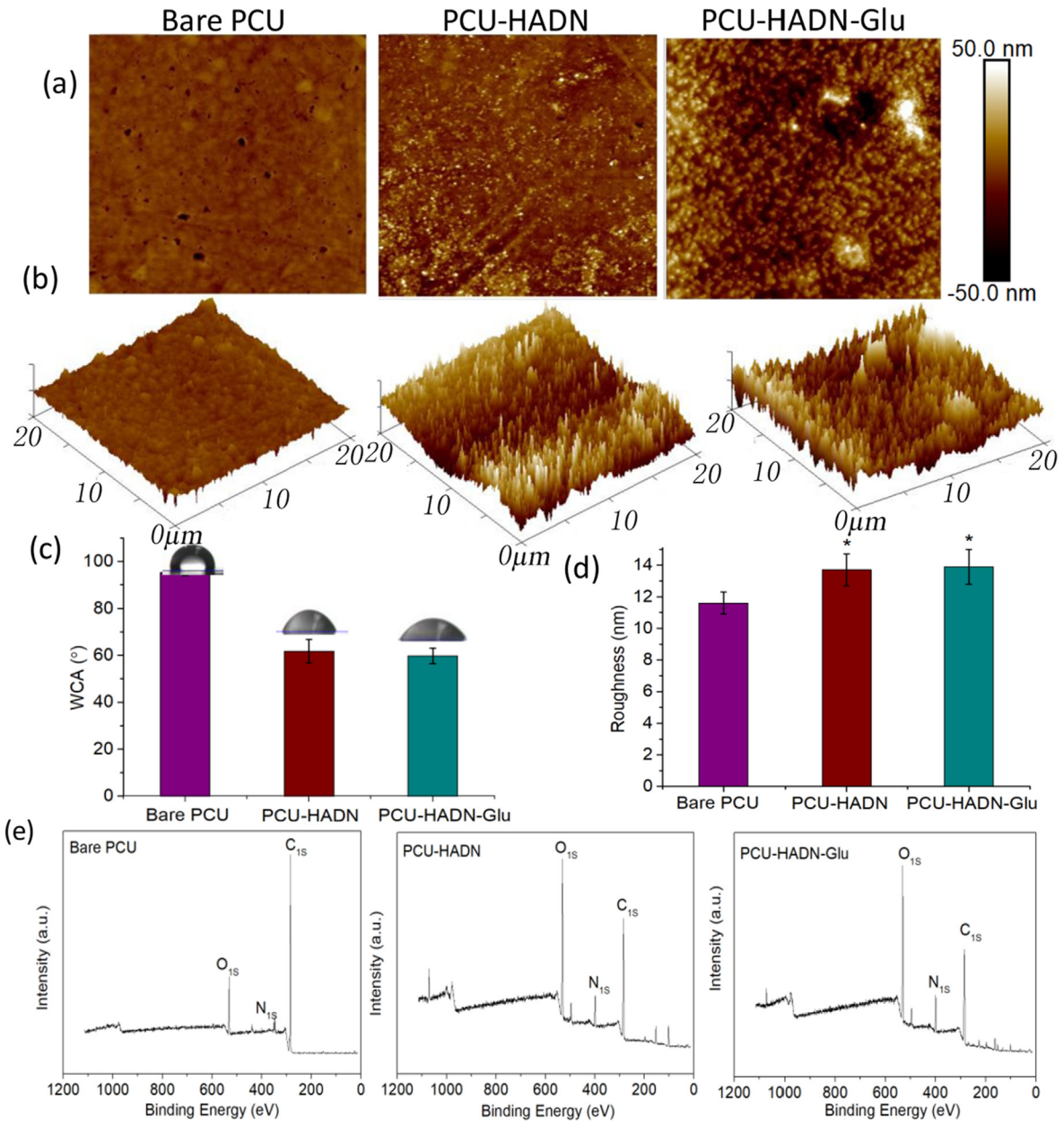

Fig. 2. Surface characterization of PCU, PCU-HADN and PCU-HADN-Glu. (a) Surface topography of each surface was measured by AFM with a scan area of 20 μm × 20 μm. (b) 3D images of each surface. (c) Surface hydrophilicity by water contact angle measurement. (d) Surface roughness. (e) The XPS analysis surface of bare PCU, PCU-HADN and PCU-HADN-Glu. Error bars represent the standard deviation over three independent measurements. Statistically significant (two tailed Student *t*-test) differences in water contact angle and roughness of PCU-HADN and PCU-HADN-Glu compared to bare PCU. * $p < 0.05$ and ** $p < 0.01$.

Table 1
Surface chemical composition of each surface. The standard deviation was calculated from three independent experiments. Values are the mean ± SD.

Samples	Atomic percentages (%)			
	C	N	O	N/C
Bare PCU	80.4 ± 2.9	1.3 ± 0.07	13 ± 1.4	1.6 ± 0.1
HADN	51.5 ± 2.9	7.6 ± 0.5	26.0 ± 1.7	14.9 ± 0.3
HADN - Glu	48.0 ± 2.1	9.8 ± 1.8	27.3 ± 1.6	20.5 ± 3.8

absorbed by one of the sliding surfaces in the form of wear or surface injury [39,55]. A typical Ft-D curve plotted every 10 min is shown in Fig. 3c; the area value can be calculated by applying the definite integral algorithm [35]. Notably, a typical Ft-D curve should have both negative and positive friction across four quadrants. It was shifted artificially to the first quadrant to calculate the absolute area value in Fig. 3c. Although the curve is similar to the shape of a parallelogram at each reciprocating cycle, the area of each cycle increased with time, especially on bare PCU. Its friction energy dissipation during 60 min of sliding was 19.3 J ± 4.1 J. It decreased to 6.9 J ± 3.5 J and 3.9 J ± 0.5 J on PCU-HADN and PCU-HADN-Glu, respectively, indicating lower cartilage wear after rub-

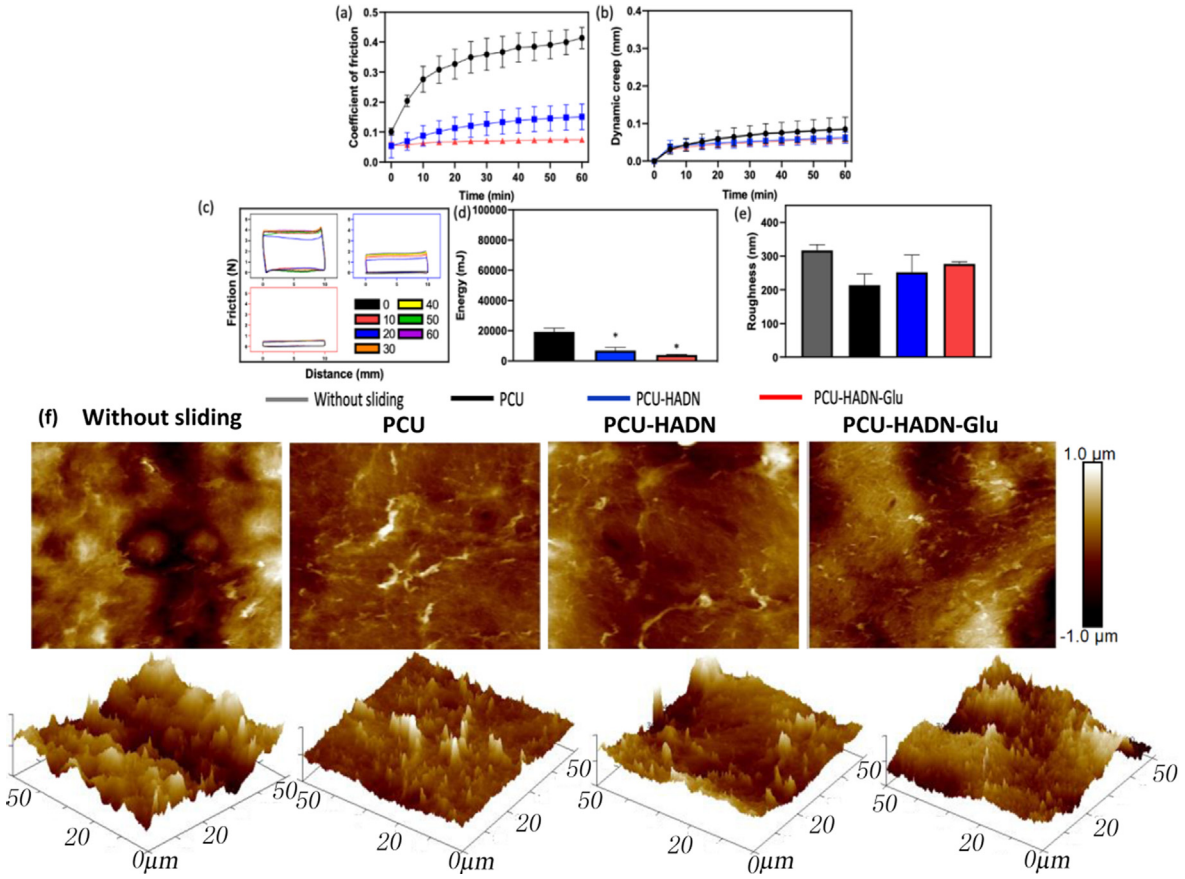

Fig. 3. Tribological performance of each PCU with rubbing against cartilage at low load (4 N). (a) The time-depended dynamic COF of cartilage rubbing against different PCU surfaces. (b) The dynamic creep of different cartilage samples with PCU. (c) Friction loop at each 10 min. (d) The entire energy dissipation. (e) Cartilage surface roughness after rubbing against each PCU. No significant differences observed. (f) Surface morphology and roughness by AFM with a scan area of 50 × 50 μm after rubbing against different PCU surfaces. Error bars represent the standard deviation over three independent measurements. Statistically significant (two tailed Student *t*-test) differences in COF and energy dissipation of PCU-HADN and PCU-HADN-Glu compared to bare PCU. *p < 0.05.

bing against PCU-HADN and PCU-HADN-Glu. The surface damage and wear were qualitatively confirmed by AFM as shown in Fig. 3e and f, where a rough pristine surface is visible for fresh cartilage with a roughness of 317 nm ± 30 nm. After the sliding, the signs of wear are visible and indicated by the red arrows in Fig. 4f. Much lower roughness of 214 nm ± 58 nm was observed on the cartilage surface after rubbing with PCU: 252 nm ± 89 nm for PCU-HADN and 277 nm ± 11 nm for PCU-HADN-Glu. Besides the roughness, the surface topography in Figs. 3f and 4f also shows the clear advantage of the coating on the PCU surface. During the AFM measurement, a low constant normal force of 5 nN was applied, and the cartilage was fixated. Thus the tactile measurement of roughness would be affected by wear caused by the reciprocating sliding against PCU rather than the damage caused by the AFM tip. The decreased roughness of cartilage after rubbing could be caused by the contact pressure during the sliding. During the sliding process, the friction caused the shear effect between PCU and cartilage surface, leading to smoothing of cartilage surface and stable phase of COF, as shown in Fig. 3a. A similar phenomenon was observed by Li et al. [55], who reported than in a certain period of time the friction decreases the roughness of skin and the lumen of the small intestine. Although no significant different in roughness was found after sliding on various surfaces, the similar roughness of cartilage after rubbing against PCU-HADN-Glu with native cartilage (without rubbing) indicates that HADN-Glu maintains better lubrication and prevents the further deformation of cartilage.

At 4 N, and right at the start the COF of cartilage against PCU, PCU-HADN and PCU-HADN-Glu is low – in the range of 0.05–0.1 – indicating that the lubrication is provided mainly by the release of interstitial fluid. Subsequently, the creep increases quickly (Fig. 3b) and continuously for 60 min on all three surfaces. Which according to Eq. (1) and Ateshian et al. [22,52] would mean increasing proportion of normal load supported by solid–solid contact and a continuous increase in COF. But this increase is only observed for bare PCU, leading to large friction energy dissipation and cartilage surface wear (Fig. 3). On the other hand, for coated PCU, i.e., PCU-HADN and PCU-HADN-Glu the COF remains significantly lower throughout the 60 min (Fig. 3a) due to the enhanced boundary lubrication. HADN-Glu decreased the COF even further due to the water retention by Glu. After modifying HADN with zwitterionic Glu, the improved lubrication yielded a lower constant COF. (Fig. 5). Previous research showed that Glu coupled to HA resulted in better antifouling performance induced by zwitterionic Glu with strong surface hydration [36]. In the present study we observed for the first time that Glu coupled to HADN can also enhance boundary lubrication against a cartilage surface.

At high loads (40 N) and at the start of sliding, the COF is significantly lower (~0.025, Fig. 4a) than at 4 N. The weeping lubrication [3,4] is more efficient at higher load, although the COF (Fig. 4a) and creep (Fig. 4b) both rise rapidly, indicating the depressurization of cartilage. Creep at 40 N was threefold larger than at 4 N but was similar for all the three surfaces. This indicates that the HADN and HADN-Glu coatings does not affect the cartilage creep behav-

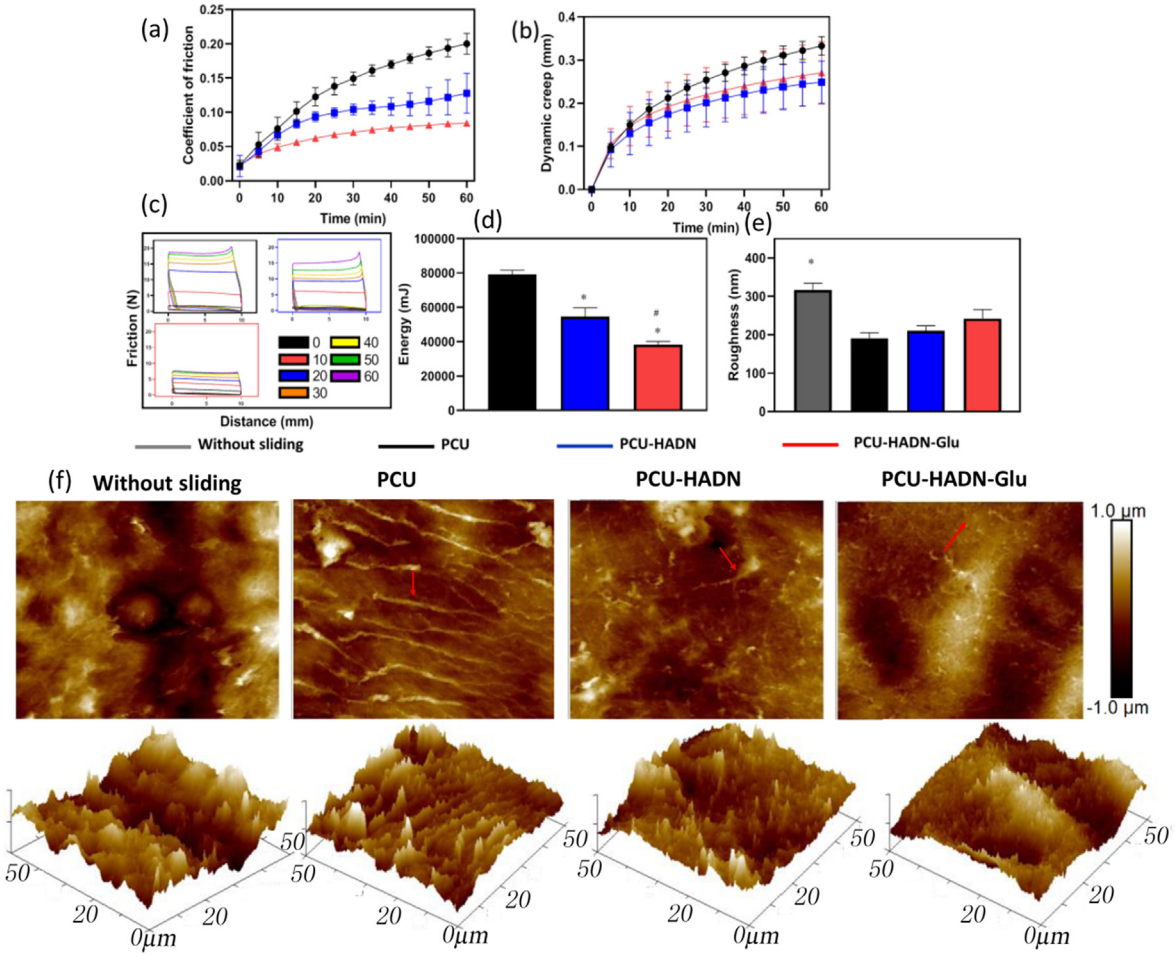

Fig. 4. Tribological performance of each PCU rubbing against cartilage at high load (40 N). (a) The time-depended dynamic COF of cartilage rubbing against different PCU surfaces. (b) The dynamic creep of different cartilage samples with PCU. (c) Friction loop at each 10 min. (d) The entire energy dissipation. (e) Cartilage surface roughness after rubbing against each PCU. * stands for statistically significant difference ($p < 0.05$) in roughness of native cartilage (without rubbing) compared to cartilage after rubbing against all PCU surfaces. (f) Surface morphology and roughness by AFM with a scan area of 50 × 50 μm after rubbing against different PCU surfaces. Error bars represent the standard deviation over three independent measurements. Statistically significant (two tailed Student *t*-test) differences in COF and energy dissipation of PCU-HADN and PCU-HADN-Glu compared to bare PCU. *$p < 0.05$. #the significant difference between cartilage rubbing against PCU-HADN-Glu and PCU-HADN.

ior, which is only load dependent. Fig. 4a shows an increase in COF on bare PCU to 0.2 ± 0.03 after 60 min of sliding, but this is lower than at 4 N (Fig. 3a). The COF of PCU coated with HADN and HADN-Glu decreased to 0.12 ± 0.05 and 0.08 ± 0.006, respectively, similar to the COF observed at 4 N. The calculation of frictional energy loss in the process of reciprocal sliding friction is shown in Fig. 4c and presented in **4d**. On bare PCU samples, the energy dissipation was 79 J ± 4.3 J after 1 h of sliding, which decreased to 54.4 J ± 9 J by coating the PCU with HADN and to 38.5 J ± 3 J by coating with HADN-Glu. The frictional energy losses are higher than 4 N despite similar COFs due to higher frictional forces caused by tenfold larger applied normal loads. After sliding, obvious abrasion was also found (indicated by the red arrows on Fig. 4e).

Insignificant decrease in roughness was observed for cartilage rubbed against bare PCU (191 nm ± 25 nm), for PCU-HADN (210 nm ± 25 nm) and for PCU-HADN-Glu (242 nm ± 41 nm), as compared to fresh cartilage at 4 N (Fig. 3e). The decrease becomes significant at 40 N (Fig. 4e). Change in roughness and surface topography (Figs. 3f and 4f) of cartilage after rubbing against PCU constitutes an abnormal and probably permanent change in the cartilage surface, which can lead to cartilage wear and degradation in the long run. Cartilage sliding against HADN-Glu coated PCU (PCU-HADN-Glu) shows least changes (both at 4 and 40 N) on the cartilage surface indicating that high lubrication abilities make it the most chondroprotective.

PCU with HADN and HADN-Glu coatings showed a tendency to reduce not only the COF but also friction energy dissipation at both loads. The HADN-Glu coating resulted in the lowest COF and energy dissipation at both 4 N and 40 N. This phenomenon is caused the synergistic effect of Glu and HADN with a strong water interaction, thus generating improved boundary lubrication (Fig. 5). In the supplementary information (Fig. S3 and S4) we show that increased surface wettability or hydrophilicity alone is not enough for a coating to provide boundary lubrication. Majd et al. [4] used a protocol to mimic the gait cycle in which both low load 4 N (swing phases) and high load 40 N (stance phases) were included in the reciprocating motion. In the present study, we separated the two phases to understand the different tribological behavior at low load and high load. Notably, at low loads (4 N) the COF between bare PCU and cartilage increased gradually up to 0.41 ± 0.06 (Fig. 3), which is similar to the observation of Majd et al. [4,24]. But our observation differed at high load, which might be caused by the more efficient weeping lubrication at high load. Glu takes the role of zwitterionic phospholipids, and HADN takes

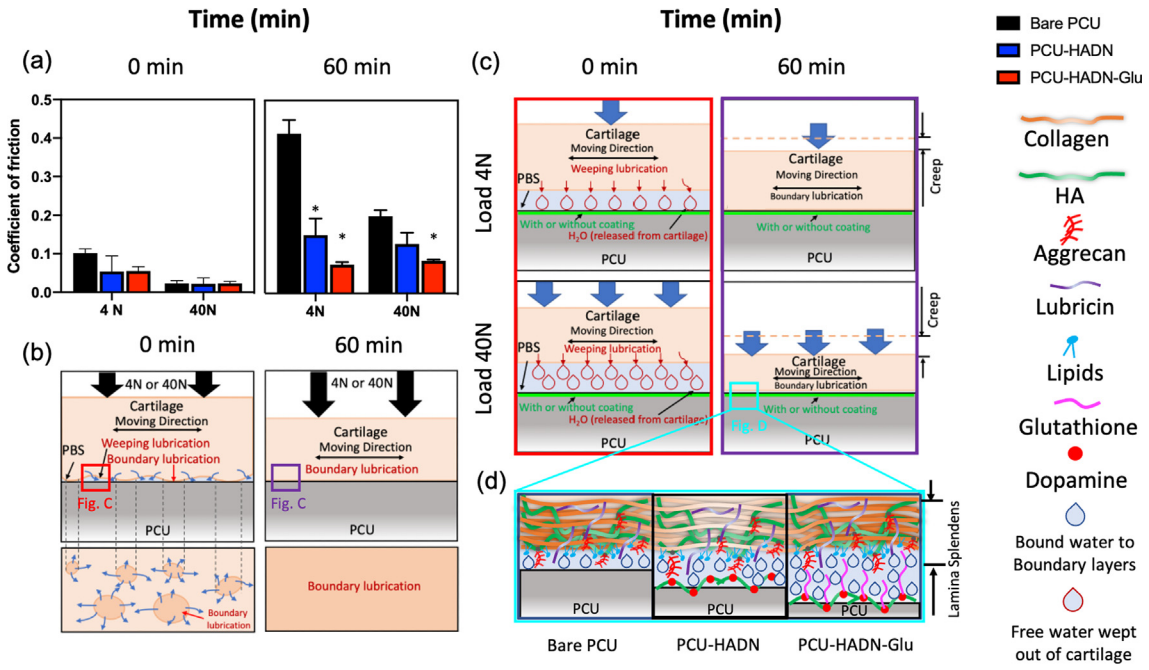

Fig. 5. Schematic illustration explaining the mechanism by which the HADN and HADN-Glu coating lubricates the PCU while sliding against cartilage. (a) The COF both at swing (4 N) and stance (40 N) phase with sliding at the start of sliding (0 min) and after 60 min, respectively. Error bars represent the standard deviation over three independent measurements. No significant difference was observed between bare and coated PCU at the beginning due to the weeping lubrication and thick fluid film formation between the cartilage and PCU. At 60 min, the significantly lower COF was detected on the PCU-HADN and PCU-HADN-Glu compared to the bare PCU (*; $P < 0.05$) at both 4 N and 40 N due to the enhanced boundary lubrication provided by the coating. (b) Cartilage-PCU contact zone, the model is taken from [56]. At the start (0 min) due to weeping the interstitial fluid flows (shown as blue arrows) into small gaps between cartilage and PCU disk as free water (shown as red drops). While sliding, creep increases as interstitial fluid flows out of cartilage, resulting in more and more small gaps disappearing where cartilage contacts PCU directly [52]. After 60 min, in the contact zone, most of the cartilage surface comes in direct contact with PCU where boundary lubrication plays important role. (c) shows the fate of the small gaps at cartilage-PCU interface which are fluid (free water) filled at the start (0 min) but disappear at 60 min both in stance (40 N) and swing phase (4 N). Since time 0 starts after 20 s of preloading we expect the cartilage to already start getting compressed and at 40 N gives rise to larger fluid filled gaps as compare to 4 N. (d) At 60 min of sliding all the free water (red drops) have flown away from the contact zone leaving bound water (blue drops) associated either with the cartilage lamina splendens or the HADN and HADN-Glu coating on the PCU surface. Bound water provides boundary lubrication, where HADN-Glu is more efficient in immobilizing (bound) water on the PCU surface than HADN or bare PCU, resulting in a lower COF as shown in (a) at 60 min. (For interpretation of the references to colour in this figure legend, the reader is referred to the web version of this article.)

the role of immobilized HA, similar to the lamina splendens in the cartilage surface, and work synergistically [5,10] to enhance boundary lubrication on the PCU biomaterial (PCU) surface.

3.4. Cell behavior on different surfaces

In terms of the specific location where sliding and friction naturally occur, it is essential to check the biocompatibility of the coating. To this end, we co-cultured the film with chondrocytes cell for one week. The chondrocyte cells were seeded on glass (ϕ 15 mm) that fit into 24 cell culture plates with or without HADN or HADN-Glu coating. On each sample, 5×10^4 cells/well were seeded and cultured by high glucose DMEM, 10% FBS, and 1% penicillin – streptomycin at 37 °C in a humidified air atmosphere of 5% CO_2; the medium changed every 3–4 days. The overview images (Fig. 6a) on each surface clearly show more cell surface coverage after day 3 compared to day 1. A significant difference in metabolic activity of cells at day 3 was observed and is shown in Fig. 6b. No significant difference in chondrocyte metabolic activity was observed between day 1 and day 7 on different surfaces. The significant difference observed on day 3 but not on day 7 could be due to the limited space for each cell, with the numbers of cells increasing after 7 days. The film of HADN and HADN-Glu with certain roughness and hydrophilicity (Fig. 3) showed high biocompatibility, which is in agreement with a study on cell-responsive enhancement by catechol active groups [30]. The high biocompatibility of the film suggests that there is no toxicity in lubrication applications.

4. Conclusion

In the study, we present a facile nanostructured coating based on HADN and Glu, which shows a distinct advantage in PCU surface lubrication. At the start of sliding the cartilage – PCU (both coated and uncoated) is lubricated by weeping lubrication, evidenced by creep. After 60 min and considerable creep, the coated PCU remains well lubricated against the cartilage at low (4 N) and high (40 N) loads, where uncoated PCU does not. This indicates that presence of HADN and HADN-Glu gives rise to boundary lubrication which keeps the COF and frictional energy low even after 60 min of creep and cartilage depressurization. HADN-Glu performs better in lubricating the PCU surface than HADN. Similar to lipids and HA in cartilage lamina splendens, in the HADN-Glu coating the zwitterionic Glu and HA play an important role in boundary lubrication. Additionally, the HADN-Glu film shows high biocompatibility, indicating that it could benefit the design of implants and medical devices. These findings demonstrate the possibility to enhance the lubrication function of implant/medical device with a nanostructured film. This study provides novel insights into the design and fabrication of biomimetic surface decoration that is relevant for biomaterial lubrication. Future studies to extend this coating to other tribological body sites, such as contact lenses and artificial hip joints, could be conducted *in vitro*, or

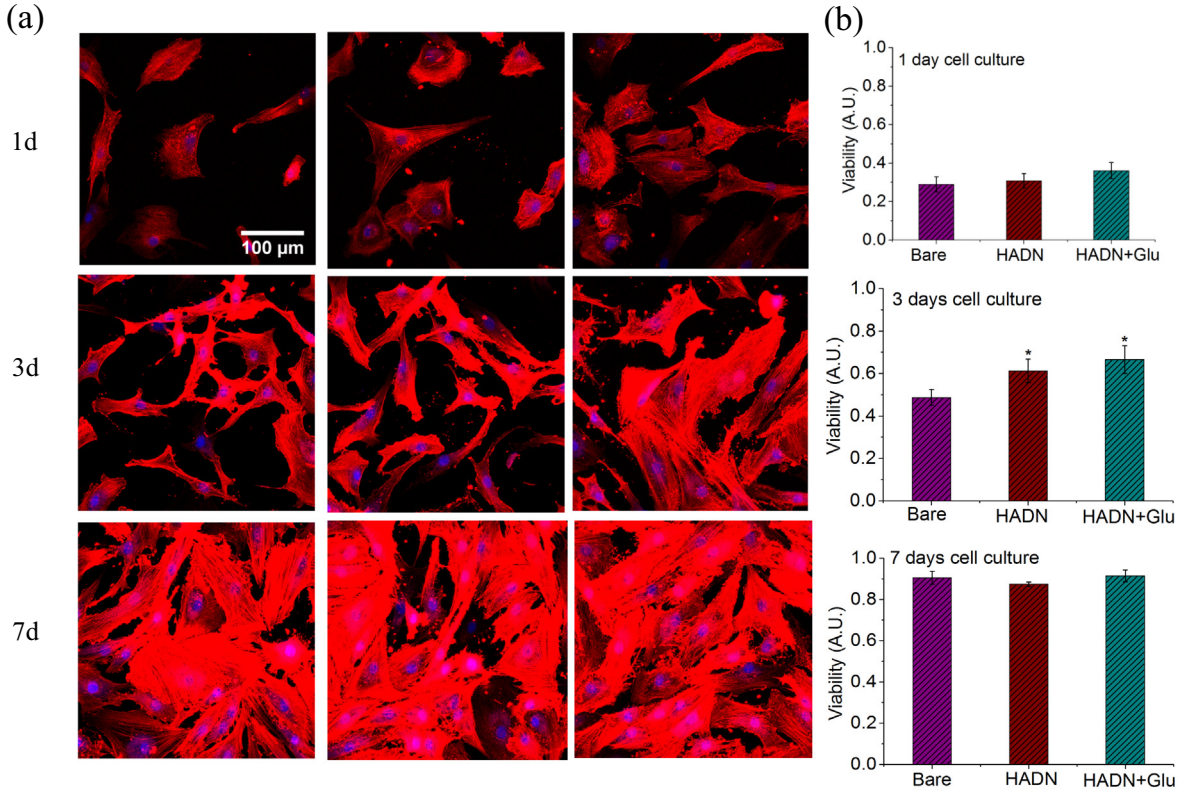

Fig. 6. Fluorescence images of cells stained with DAPI (nucleus) and TRITC-pholloaidin (cytoskeleton) for chondrocyte cells at 1, 3 and 7 days of culture. XTT analysis of the cell viability on each surface. The scale bar represents 100 μm in the first image and also for the other images. Error bars represent the standard deviation over three independent measurements. Statistically significant differences are marked with * (indicating p-value < 0.05).

in vivo to test the durability. This would help to broaden the applicability of this coating for medical devices for which lubrication is required.

Declaration of Competing Interest

The authors declare that they have no known competing financial interests or personal relationships that could have appeared to influence the work reported in this paper.

Acknowledgements

The UMT-3 tribometer (Bruker) setup was purchased thanks to the grant no. 91112026 from the Netherlands Organization for Health Research and Development (ZonMW). We also would like to thank the China Scholarship Council for a 4 year scholarship to Drs. H. Wan (project no. 201606320244) and Drs. K. Ren (project no. CSC201806400039) to pursue their Ph.D.

Appendix A. Supplementary material

Supplementary data to this article can be found online at https://doi.org/10.1016/j.jcis.2021.03.052.

References

[1] H. Wan, A. Vissink, P.K. Sharma, Enhancement in Xerostomia Patient Salivary Lubrication Using a Mucoadhesive, J. Dent. Res. 99 (2020) 914–921, https://doi.org/10.1177/0022034520917675.
[2] H. Wan, C. Ma, J. Vinke, A. Vissink, A. Herrmann, P.K. Sharma, Next generation salivary lubrication enhancer derived from recombinant supercharged polypeptides for Xerostomia, ACS Appl. Mater. Interfaces 12 (2020) 34524–34535, https://doi.org/10.1021/acsami.0c06159.
[3] C.W. McCutchen, The frictional properties of animal joints, Wear 5 (1962) 1–17, https://doi.org/10.1016/0043-1648(62)90176-X.
[4] S.E. Majd, A.I. Rizqy, H.J. Kaper, T.A. Schmidt, R. Kuijer, P.K. Sharma, An in vitro study of cartilage–meniscus tribology to understand the changes caused by a meniscus implant, Colloids Surf. B Biointerfaces 155 (2017) 294–303, https://doi.org/10.1016/j.colsurfb.2017.04.034.
[5] S. Jahn, J. Seror, J. Klein, Lubrication of articular cartilage, Annu. Rev. Biomed. Eng. 18 (2016) 235–258, https://doi.org/10.1146/annurev-bioeng-081514-123305.
[6] L. Zhu, J. Seror, A.J. Day, N. Kampf, J. Klein, Ultra-low friction between boundary layers of hyaluronan-phosphatidylcholine complexes, Acta Biomater. 59 (2017) 283–292, https://doi.org/10.1016/j.actbio.2017.06.043.
[7] K.A. Athanasiou, E.M. Darling, G.D. DuRaine, J.C. Hu, A.H. Reddi, Articular cartilage, second ed., CRC Press, Boca Raton, FL, 2017.
[8] A. Singh, M. Corvelli, S.A. Unterman, K.A. Wepasnick, P. McDonnell, J.H. Elisseeff, Enhanced lubrication on tissue and biomaterial surfaces through peptide-mediated binding of hyaluronic acid, Nat. Mater. 13 (2014) 988–995, https://doi.org/10.1038/nmat4048.
[9] A. Raj, M. Wang, T. Zander, D.C.F. Wieland, X. Liu, J. An, V.M. Garamus, R. Willumeit-Römer, M. Fielden, P.M. Claesson, A. De ˙ Dinaite, Lubrication synergy: mixture of hyaluronan and dipalmitoylphosphatidylcholine (DPPC) vesicles, J. Colloid Interface Sci. 488 (2017) 225–233. https://doi.org/10.1016/j.jcis.2016.10.091.
[10] J. Seror, L. Zhu, R. Goldberg, A.J. Day, J. Klein, Supramolecular synergy in the boundary lubrication of synovial joints, Nat. Commun. 6 (2015) 6497, https://doi.org/10.1038/ncomms7497.
[11] K.A. Waller, L.X. Zhang, K.A. Elsaid, B.C. Fleming, M.L. Warman, G.D. Jay, Role of lubricin and boundary lubrication in the prevention of chondrocyte apoptosis, Proc. Natl. Acad. Sci. 110 (2013) 5852–5857, https://doi.org/10.1073/pnas.1219289110.
[12] G.D. Jay, K.A. Waller, The biology of Lubricin: Near frictionless joint motion, Matrix Biol. 39 (2014) 17–24, https://doi.org/10.1016/J.MATBIO.2014.08.008.
[13] J. Klein, Molecular mechanisms of synovial joint lubrication, Proc. Inst. Mech. Eng. Part J J. Eng. Tribol. 220 (2006) 691–710, https://doi.org/10.1243/13506501JET143.
[14] A. Raj, M. Wang, C. Liu, L. Ali, N.G. Karlsson, P.M. Claesson, A. De Dinaite, Molecular synergy in biolubrication: The role of cartilage oligomeric matrix protein (COMP) in surface-structuring of lubricin, J. Colloid Interface Sci. 495 (2017) 200–206. https://doi.org/10.1016/j.jcis.2017.02.007.
[15] B. Zappone, G.W. Greene, E. Oroudjev, G.D. Jay, J.N. Israelachvili, Molecular aspects of boundary lubrication by human lubricin: effect of disulfide bonds and enzymatic digestion, Langmuir 24 (2008) 1495–1508.

[16] G.W. Greene, X. Banquy, D. Woog, D.D. Lowrey, J. Yu, J.N. Israelachvili, Adaptive mechanically controlled lubrication mechanism found in articular joints, PNAS 108 (2011) 5255–5259, https://doi.org/10.1073/pnas.1101002108.
[17] J. Charnley, The lubrication of animal joints in relation to surgical reconstruction by arthroplasty, Ann. Rheum. Dis. 19 (1960) 10–19.
[18] B.D. Ratner, A.S. Hoffman, F.J. Schoen, J.E. Lemons, Biomaterials Science: An Introduction to Materials in Medicine, Elsevier Acad. Press (2004) 137–152. doi:B978-0-08-087780-8.00035-8.
[19] J.J. Nichols, L. Jones, J.D. Nelson, F. Stapleton, D.A. Sullivan, M.D.P. Willcox, The TFOS International Workshop on Contact Lens Discomfort: Introduction, Investig. Opthalmology Vis. Sci. 54 (2013) TFOS1. https://doi.org/10.1167/iovs.13-13195.
[20] J.J. Nichols, M.D.P. Willcox, A.J. Bron, C. Belmonte, J.B. Ciolino, J.P. Craig, M. Dogru, G.N. Foulks, L. Jones, J.D. Nelson, K.K. Nichols, C. Purslow, D.A. Schaumberg, F. Stapleton, D.A. Sullivan, the members of the T.I.W. on C.L. Discomfort, The TFOS international workshop on contact lens discomfort: executive summary, Invest. Ophthalmol. Vis. Sci. 54 (2013) TFOS7, https://doi.org/10.1167/IOVS.13-13212.
[21] H. Wan, C. Lin, H.J. Kaper, P.K. Sharma, A polyethylene glycol functionalized hyaluronic acid coating for cardiovascular catheter lubrication, Mater. Des. 196 (2020) 109080, https://doi.org/10.1016/j.matdes.2020.109080.
[22] M. Caligaris, G.A. Ateshian, Effects of sustained interstitial fluid pressurization under migrating contact area, and boundary lubrication by synovial fluid, on cartilage friction, Osteoarthritis Cartilage 16 (2008) 1220–1227, https://doi.org/10.1016/j.joca.2008.02.020.
[23] S.P. Ho, N. Nakabayashi, Y. Iwasaki, T. Boland, M. LaBerge, Frictional properties of poly(MPC-co-BMA) phospholipid polymer for catheter applications, Biomaterials (2003), https://doi.org/10.1016/S0142-9612(03)00450-2.
[24] S.E. Majd, R. Kuijer, T.A. Schmidt, P.K. Sharma, Role of hydrophobicity on the adsorption of synovial fluid proteins and biolubrication of polycarbonate urethanes: materials for permanent meniscus implants, Mater. Des. 83 (2015) 514–521, https://doi.org/10.1016/j.matdes.2015.06.075.
[25] J. Seror, R. Sorkin, J. Klein, Boundary lubrication by macromolecular layers and its relevance to synovial joints, Polym. Adv. Technol. 25 (2014) 468–477, https://doi.org/10.1002/pat.3295.
[26] M. Wang, C. Liu, E. Thormann, A. Dedinaite, Hyaluronan and phospholipid association in biolubrication, Biomacromolecules 14 (2013) 4198–4206, https://doi.org/10.1021/bm400947v.
[27] S. Sivan, A. Schroeder, G. Verberne, Y. Merkher, D. Diminsky, A. Priev, A. Maroudas, G. Halperin, D. Nitzan, I. Etsion, Y. Barenholz, Liposomes act as effective biolubricants for friction reduction in human synovial joints, Langmuir 26 (2010) 1107–1116, https://doi.org/10.1021/la9024712.
[28] S. Hong, K. Yang, B. Kang, C. Lee, I.T. Song, E. Byun, K.I. Park, S.W. Cho, H. Lee, Hyaluronic acid catechol: a biopolymer exhibiting a pH-dependent adhesive or cohesive property for human neural stem cell engineering, Adv. Funct. Mater. 23 (2013) 1774–1780, https://doi.org/10.1002/adfm.201202365.
[29] A.I. Neto, N.L. Vasconcelos, S.M. Oliveira, D. Ruiz-Molina, J.F. Mano, High-throughput topographic, mechanical, and biological screening of multilayer films containing mussel-inspired biopolymers, Adv. Funct. Mater. 26 (2016) 2745–2755, https://doi.org/10.1002/adfm.201505047.
[30] A.I. Neto, A.C. Cibrão, C.R. Correia, R.R. Carvalho, G.M. Luz, G.G. Ferrer, G. Botelho, C. Picart, N.M. Alves, J.F. Mano, Nanostructured polymeric coatings based on chitosan and dopamine-modified hyaluronic acid for biomedical applications, Small 10 (2014) 2459–2469, https://doi.org/10.1002/smll.201303568.
[31] J.B. Schlenoff, Zwitteration: coating surfaces with zwitterionic functionality to reduce nonspecific adsorption, Langmuir 30 (2014) 9625–9636, https://doi.org/10.1021/la500057j.
[32] Z. Wang, J. Li, Y. Liu, J. Luo, Macroscale superlubricity achieved between zwitterionic copolymer hydrogel and sapphire in water, Mater. Des. 188 (2020) 108441, https://doi.org/10.1016/J.MATDES.2019.108441.
[33] H. Nakano, Y. Noguchi, S. Kakinoki, M. Yamakawa, I. Osaka, Y. Iwasaki, Highly durable lubricity of photo-cross-linked zwitterionic polymer brushes supported by poly(ether ether ketone) substrate, ACS Appl. Bio Mater. 3 (2020) 1071–1078, https://doi.org/10.1021/acsabm.9b01040.
[34] Y. Zheng, J. Yang, J. Liang, X. Xu, W. Cui, L. Deng, H. Zhang, Bioinspired hyaluronic acid/phosphorylcholine polymer with enhanced lubrication and anti-inflammation, Biomacromolecules 20 (2019), https://doi.org/10.1021/acs.biomac.9b00964.
[35] E. Scoppola, A. Sodo, S.E. McLain, M.A. Ricci, F. Bruni, Water-peptide site-specific interactions: a structural study on the hydration of glutathione, Biophys. J. 106 (2014) 1701–1709, https://doi.org/10.1016/j.bpj.2014.01.046.
[36] H. Ye, Y. Xia, Z. Liu, R. Huang, R. Su, W. Qi, L. Wang, Z. He, Dopamine-assisted deposition and zwitteration of hyaluronic acid for nanoscale fabrication of low-fouling surfaces, J. Mater. Chem. B 4 (2016) 4084–4091, https://doi.org/10.1039/C6TB01022A.
[37] H. Wan, X. Zhao, C. Lin, H.J. Kaper, P.K. Sharma, Nanostructured coating for biomaterial lubrication through biomacromolecular recruitment, ACS Appl. Mater. Interfaces 12 (2020) 23726–23736, https://doi.org/10.1021/acsami.0c04899.
[38] S.M. Horvath, J.L. Hollander, Intra-articular temperature as a measure of joint reaction, J. Clin. Invest. 28 (1949) 469–473, https://doi.org/10.1172/JCI102092.
[39] W. Li, L. Shi, H. Deng, Z. Zhou, Investigation on friction trauma of small intestine in vivo under reciprocal sliding conditions, Tribol. Lett. 55 (2014) 261–270, https://doi.org/10.1007/s11249-014-0356-6.
[40] R. Kuijer, P. Emans, E. Jansen, M. Hulsbosch, D. Surtel, S. Bulstra, Isolation and cultivation of Chondrogenic Precursors From Aged Human Periosteum 49th Annual Meeting of the Orthopaedic Research Society Paper # 0101, 67 (n.d.) 101.
[41] H. Wan, K. Ren, H.J. Kaper, P.K. Sharma, A bioinspired mucoadhesive restores lubrication of degraded cartilage through reestablishment of lamina splendens, Colloids Surf. B Biointerfaces 193 (2020) 110977, https://doi.org/10.1016/J.COLSURFB.2020.110977.
[42] H. Lee, Y. Lee, A.R. Statz, J. Rho, T.G. Park, P.B. Messersmith, Substrate-independent layer-by-layer assembly by using mussel-adhesive- inspired polymers, Adv. Mater. 20 (2008) 1619–1623, https://doi.org/10.1002/adma.200702378.
[43] W. Xu, J. Qian, G. Hou, A. Suo, Y. Wang, J. Wang, T. Sun, M. Yang, X. Wan, Y. Yao, Hyaluronic acid-functionalized gold nanorods with pH/NIR dual-responsive drug release for synergetic targeted photothermal chemotherapy of breast cancer, ACS Appl. Mater. Interfaces 9 (2017) 36533–36547, https://doi.org/10.1021/acsami.7b08700.
[44] A. Singh, J. Zhan, Z. Ye, J.H. Elisseeff, Modular multifunctional poly(ethylene glycol) hydrogels for stem cell differentiation, Adv. Funct. Mater. 23 (2013) 575–582, https://doi.org/10.1002/adfm.201201902.
[45] K. Kim, K. Kim, J.H. Ryu, H. Lee, Chitosan-catechol: A polymer with long-lasting mucoadhesive properties, Biomaterials 52 (2015) 161–170, https://doi.org/10.1016/J.BIOMATERIALS.2015.02.010.
[46] Y. Li, M. Qin, Y. Li, Y. Cao, W. Wang, Single molecule evidence for the adaptive binding of DOPA to different wet surfaces, Langmuir 30 (2014) 4358–4366, https://doi.org/10.1021/la501189n.
[47] S.E. Majd, R. Kuijer, A. Köwitsch, T. Groth, T.A. Schmidt, P.K. Sharma, Both hyaluronan and collagen type II keep proteoglycan 4 (lubricin) at the cartilage surface in a condition that provides low friction during boundary lubrication, Langmuir 30 (2014) 14566–14572, https://doi.org/10.1021/la504345c.
[48] G. Zur, E. Linder-Ganz, J.J. Elsner, J. Shani, O. Brenner, G. Agar, E.B. Hershman, S. P. Arnoczky, F. Guilak, A. Shterling, Chondroprotective effects of a polycarbonate-urethane meniscal implant: histopathological results in a sheep model, Knee Surg. Sports Traumatol. Arthrosc. 19 (2011) 255–263, https://doi.org/10.1007/s00167-010-1210-5.
[49] J. Klompmaker, R.P.H. Veth, H.W.B. Jansen, H.K.L. Nielsen, J.H. De Groot, A.J. Pennings, Meniscal replacement using a porous polymer prosthesis: a preliminary study in the dog, Biomaterials 17 (1996) 1169–1175, https://doi.org/10.1016/0142-9612(96)84937-4.
[50] A.C.T. Vrancken, W. Madej, G. Hannink, N. Verdonschot, T.G. van Tienen, P. Buma, Short term evaluation of an anatomically shaped polycarbonate urethane total meniscus replacement in a goat model, PLoS One 10 (2015) e0133138, https://doi.org/10.1371/journal.pone.0133138.
[51] A.C.T. Vrancken, T.G. van Tienen, G. Hannink, D. Janssen, N. Verdonschot, P. Buma, Releasing the circumferential fixation of the medial meniscus does not affect its kinematics, Knee 21 (2014) 1033–1038, https://doi.org/10.1016/j.knee.2014.08.006.
[52] G.A. Ateshian, The role of interstitial fluid pressurization in articular cartilage lubrication, J. Biomech. 42 (2009) 1163–1176, https://doi.org/10.1016/j.jbiomech.2009.04.040.
[53] M.A. Soltz, G.A. Ateshian, Experimental verification and theoretical prediction of cartilage interstitial fluid pressurization at an impermeable contact interface in confined compression, J. Biomech. 31 (1998) 927–934, https://doi.org/10.1016/S0021-9290(98)00105-5.
[54] T. Farquhar, P.R. Dawson, P.A. Torzilli, A microstructural model for the anisotropic drained stiffness of articular cartilage, J. Biomech. Eng. 112 (1990) 414–425, https://doi.org/10.1115/1.2891205.
[55] W. Li, Q. Pang, M. Lu, Y. Liu, Z.R. Zhou, Rehabilitation and adaptation of lower limb skin to friction trauma during friction contact, Wear 332–333 (2015) 725–733, https://doi.org/10.1016/j.wear.2015.01.045.
[56] A.C. Moore, D.L. Burris, Tribological rehydration of cartilage and its potential role in preserving joint health, Osteoarthr. Cartil. 25 (2017) 99–107, https://doi.org/10.1016/j.joca.2016.09.018.